

Groupe d'Annecy

Laboratoire
d'Annecy-le-Vieux de
Physique des Particules

ENSLAPP

Groupe de Lyon

Ecole Normale
Supérieure de Lyon

Inclusive hard processes in photon induced reactions ^{*}

P. Aurenche¹

Laboratoire de Physique Théorique ENSLAPP[†]

¹ Groupe d'Annecy: LAPP, BP 110, F-74941 Annecy-le-Vieux Cedex, France.

Abstract

In the following some aspects of inclusive hard processes in photon induced reactions are reviewed. After a discussion on the properties of hard processes, the phenomenology of jet production and of charmonium production is presented in the context of the next-to-leading logarithm approximation of QCD.

hep-ph/yymmnn
ENSLAPP-A-652/97
May 1997

^{*}Talk presented at PHOTON '97, Egmond aan Zee, The Netherlands, May 1997

[†]URA 14-36 du CNRS, associée à l'Ecole Normale Supérieure de Lyon et à l'Université de Savoie.

1 Introduction

Over the last few years the physics of hard processes in photon-induced reactions (*e.g.* photo-production at HERA and photon-photon collisions at TRISTAN and LEP) has almost reached the status of sophistication of hard processes in purely hadronic reactions. The experimental results are becoming more and more accurate and many observables measured in hadronic reactions are now being accessible in photon-induced reactions while the corresponding theoretical calculations have been performed at the next-to-leading order (NLO) of perturbative QCD. Since PHOTON '95 [1] an enormous progress has been made in this respect so that one should be able to start quantitative phenomenology. The main points that deserve special attention now are: 1) matching the calculated observables with the experimental ones; 2) matching the appropriate non-perturbative input to the conventions used in the NLO calculations.

It is well known that the physics of photon-induced processes is more complex than that of pure hadronic reactions. This arises from the fact that the photon acts either as a *parton* which couples directly to the hard scattering and contributes to *direct* processes, or as a *composite* object (a bag of partons) the constituents of which couple to the hard scattering via the photon structure functions: this leads to *resolved* processes. Furthermore, as discussed in ref. [2] the photon structure function contains two pieces:

$$F_{i/\gamma}(x, Q) = F_{i/\gamma}^{\text{had}}(x, Q) + F_{i/\gamma}^{\text{anom}}(x, Q), \quad i = \text{quark, gluon} \quad (1)$$

where the first term on the right hand-side is similar to the hadronic structure function while the second term increases logarithmically with Q^2 and is asymptotically calculable in perturbation theory.

In the following, in a theoretical introduction, the structure of a “typical” cross section will be derived stressing the features distinguishing the *direct* processes from the *resolved* ones. Two topics are selected for further discussion: the production of jets and single particle on the one hand and the production of hidden charm for which HERA offers the possibility to test models of J/Ψ production at the Tevatron.

2 Photon induced reactions: theory

We consider photon-photon collisions as an example. The lowest order diagram is shown in fig. 1a. To apply the perturbative approach a large scale is needed which is provided by the transverse momentum of the produced jet or the mass of the heavy quark. Considering jet production, the Born approximation is valid for large values of p_T/\sqrt{s} where unfortunately the cross section is very small since it behaves as $d\sigma^{\text{jet}}/d\vec{p}_T \sim \alpha^2/p_T^4$. To obtain reliable predictions at lower p_T values it is necessary to consider diagrams with an extra gluon emission, leading in principle, to $\mathcal{O}(\alpha_s)$ corrections to the cross section (fig. 1b,c). When integrating over the phase-space of final state partons to reconstruct *e.g.* the single inclusive jet cross section, one encounters “dangerous” regions where the virtualities of some fermion propagators may vanish and the corresponding matrix elements are not defined. This happens, for example, when the final state parton of momentum p_1 is collinear to the initial photon of momentum k_a ($s_{a_1} =$

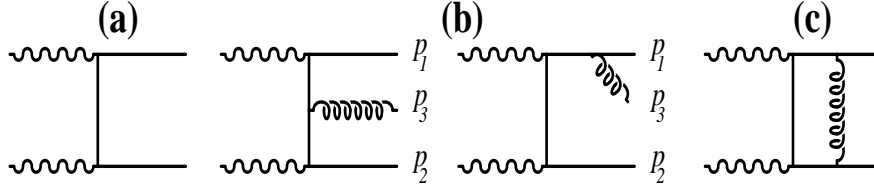


Figure 1: *Feynman diagrams for $\gamma\gamma$ scattering. (a): Born approximation; (b) real corrections; (c) virtual corrections.*

($k_a - p_1$) $^2 \rightarrow 0$) or the emitted gluon is collinear to a final state quark ($s_{13} = (p_1 + p_3)^2 \rightarrow 0$). Considering the s_{a1} singular region, the process can be pictured as in fig. 2a where the initial photon fragments into a collinear $q\bar{q}$ pair followed by the hard 2 body \rightarrow 2 body scattering of the q or \bar{q} , the other parton flying off down the beam pipe. The photon fragmentation is a soft process (the relevant scale s_{a1} is small) which takes place on a long time scale before the short-distance process scatters the partons at large transverse momenta. The cross section can be written as

$$\frac{d\sigma^{\gamma\gamma}}{d\vec{p}_T d\eta} = \int dz P_{q/\gamma}(z) \ln\left(\frac{M^2}{\lambda^2}\right) \frac{d\sigma^{\gamma q}}{d\vec{p}_T d\eta} + \frac{\alpha_s}{2\pi} K^D(p_T, M), \quad (2)$$

where λ is a cut-off introduced to regularise the collinear singularity, and $M \sim \mathcal{O}(p_T)$ is an

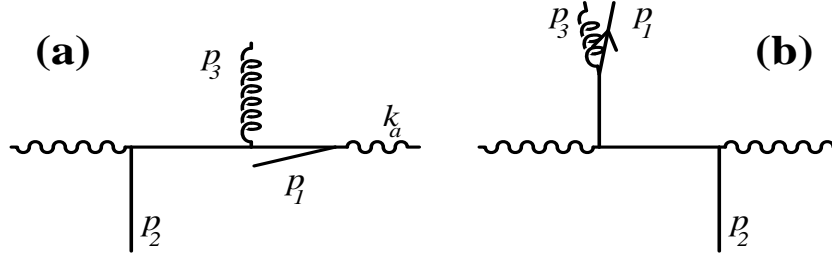


Figure 2: *Diagrammatic representation of the collinear singularities.*

arbitrary scale introduced to separate the contribution from the collinear region, generating the “large” $\ln(M^2/\lambda^2)$ piece, from the hard region (roughly $s_{a1} > M^2$) leading to the term K^D containing only finite terms such as $\ln(p_T/M^2)$. The above expression is rigourously independent of the scale M . In fact, at this level of approximation the scale M is not necessary but it is introduced for later use. The integration variable in eq. 2 is simply the fraction of the photon momentum carried by the interacting q or \bar{q} . Using the factorisation theorem, we can substitute to the “large logarithm” term $P_{q/\gamma}(z) \ln(M^2/\lambda^2)$ the photon structure function $F_{q/\gamma}(z, M)$, measured in $\gamma^*\gamma$ collisions, which satisfies evolution equations of type:

$$\frac{dF_{i/\gamma}(M)}{d \ln M^2} = P_{i\gamma} + \sum_{j=q,g} P_{ij} \otimes F_{j/\gamma}(M), \quad i, j = q, g \quad (3)$$

where the symbol \otimes denotes a convolution over the longitudinal variable and the P_{ij} are the usual splitting functions. After replacing $P_{q/\gamma} \ln(M^2/\lambda^2)$ by $F_{q/\gamma}(M)$ in eq. (2) the compensation in the M dependence on the right-hand side is only approximate as the evolution

equation effectively resums large higher order corrections (of type $[\alpha_s(M) \ln(M/\Lambda_{QCD})]^n$) in $F_{q/\gamma}(M)$ whereas no such resummation is performed in K^D . The cross section can be written

$$\frac{d\sigma^{\gamma\gamma}}{d\vec{p}_T d\eta} = \left(\frac{d\sigma^{\gamma\gamma(0)}}{d\vec{p}_T d\eta} + \frac{\alpha_s}{2\pi} K^D(p_T, M) \right) + \int dz F_{q/\gamma}(z, M) \frac{d\sigma^{\gamma q}}{d\vec{p}_T d\eta} \quad (4)$$

where the K^D term is a correction to the Born cross section $d\sigma^{\gamma\gamma(0)}$ and contributes to the *direct* cross section evaluated in the NLO approximation. The last term in the equation is the *resolved* process. Since in the latter case only part of the energy of the photon contributes to the large p_T process, the rest being carried by the longitudinal fragment, the *resolved* term is qualitatively (*i.e.* in the LO approximation) distinguished from the *direct* one by:

- a softer p_T spectrum;
- a jet system boosted in the direction opposite to that of the resolved photon: *e.g.* a backward moving resolved photon produces forward going jets;
- some hadronic activity in the direction of the resolved photon.

In the NLO approximation the *direct* and *resolved* components are *not separately observable* since they depend on the arbitrary renormalisation scale M . However, using the properties above it is possible to define observables related to these two components (see below).

Until now we have discussed features related to the initial state singularities. The final state singularities (of type $s_{13} \rightarrow 0$) also lead to 2 body \rightarrow 2 body hard scattering with the singular behaviour associated to the fragmentation process exactly as in purely hadronic processes (fig. 2b). The cross section is made finite by adding the virtual diagrams and properly defining the jets, merging the two almost collinear partons into one jet, or by convoluting with a fragmentation function and using the factorisation theorem to build the scaling violations in the fragmentation function.

One could continue the perturbative analysis and consider the emission of more partons: this will lead to *double resolved* processes where each photon interacts via its structure function. Finally, the $\gamma\gamma$ cross section for inclusive jet production takes the form:

$$\frac{d\sigma^{\gamma\gamma}}{d\vec{p}_T d\eta} = \frac{d\sigma^D}{d\vec{p}_T d\eta} + \frac{d\sigma^{SR}}{d\vec{p}_T d\eta} + \frac{d\sigma^{DR}}{d\vec{p}_T d\eta} \quad (5)$$

with the *direct*, *single resolved* and *double resolved* pieces given in the NLO approximation by an expansion of type:

$$\frac{d\sigma^D}{d\vec{p}_T d\eta}(R) = \frac{d\sigma^{\gamma\gamma(0)}}{d\vec{p}_T d\eta} + \frac{\alpha_s}{2\pi} K^D(R; p_T, M), \quad (6)$$

and similarly for the other terms. The variable R specifies the jet cone size. The factorisation scale variation associated to the inhomogeneous term $P_{i\gamma}$ in eq. (3) is compensated between the D , SR and DR pieces while the variation associated to the homogeneous terms P_{ij} compensates within each of these pieces between the lowest order and the correction terms. Thus only eq. (5) is expected to be stable under variation of scale M but not its individual components.

For hadron production an extra convolution of the above expressions with the relevant fragmentation function is needed. For photo-production processes one of the $F_{i/\gamma}(x, M)$ should be

replaced by the hadronic structure function. In an obvious notation, the cross section takes the simpler form:

$$\frac{d\sigma^{\gamma p}}{d\vec{p}_T d\eta} = \frac{d\sigma^D}{d\vec{p}_T d\eta} + \frac{d\sigma^R}{d\vec{p}_T d\eta}. \quad (7)$$

3 Phenomenology of jet production

One of the aims of studies of hard processes in γ induced reactions is the NLO determination of the photon structure function [3]. To achieve this it is very useful to isolate in an experimental way the *resolved* component of the cross section. In a *direct* process, all the photon energy is given to jets at large p_T so that by momentum conservation one has for a 2-jet event (the photon is assumed to move towards negative rapidity):

$$x_\gamma = \frac{E_{T1}e^{-\eta_1} + E_{T2}e^{-\eta_2}}{2E_\gamma} = 1 \quad (8)$$

Higher order correction are not expected to change this relation drastically. In contrast, for a *resolved* event $x_\gamma < 1$ since part of the photon energy disappears in the beam pipe (fig. 2a) (in ref. [4] a modified definition of x_γ is proposed). At HERA, the experimental groups choose the value $x_\gamma = .75$ as a cut-off so that above this value the events are produced mostly by the *direct* process while below they are mainly *resolved*. The integrated di-jet cross sections for HERA,

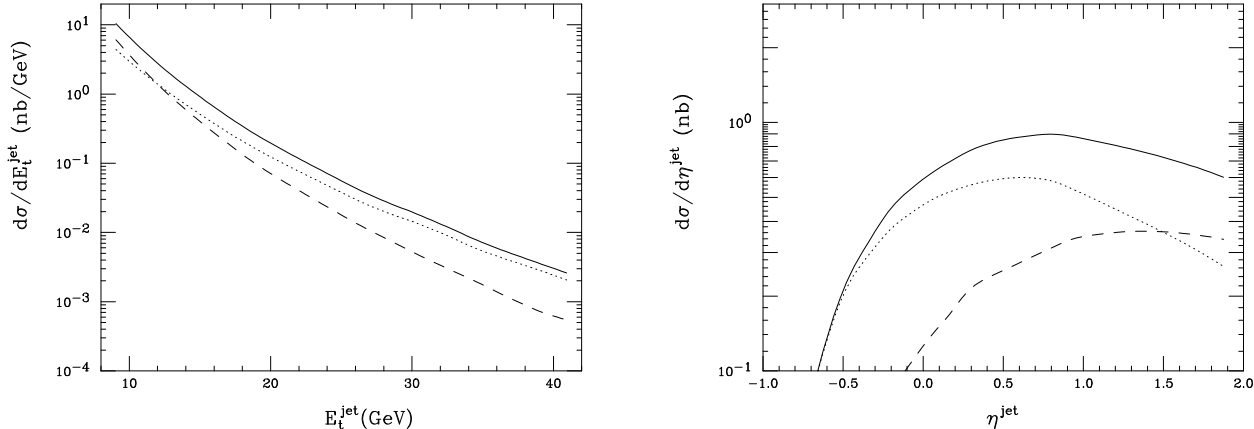


Figure 3: *Integrated di-jet cross section in the domains $0 < x_\gamma < 1$ (solid line), $x_\gamma < .75$ (dashed line), $x_\gamma > .75$ (dotted line). From ref. [5].*

shown in fig. 3, nicely illustrate, in the NLO approximation [5] the different characteristics of the two components. In the first figure the direct component shows a faster decrease with E_T , while in the second one the resolved cross section is seen to contribute mainly forward jets. In fig. 4 a very good agreement is seen, between the NLO theory [5] and experiment [6], in the shape of the di-jet angular distribution (the angle is measured in the di-jet rest frame): as expected the *resolved* component has a steeper angular dependence due to the importance of gluon exchange diagrams while for the *direct* term only quark exchange is allowed. In the next figure, we compare theoretical predictions of two independent groups [5, 7] with ZEUS

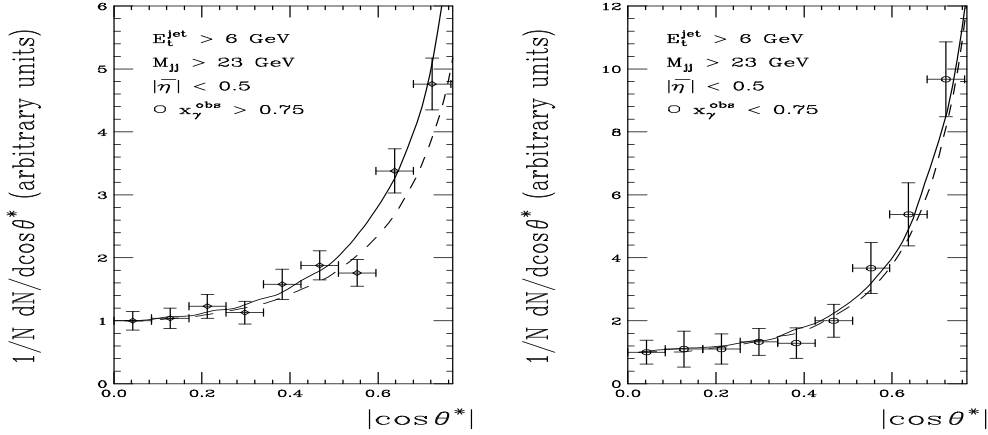


Figure 4: *Dijet angular distribution as measured by ZEUS [6] normalized to one at $\cos\theta^* = 0$ compared with LO (dash lines) and NLO result (solid lines), from ref. [5].*

data for the di-jet cross section [8] $d\sigma/d\bar{\eta}$, integrated over the phase space $E_{T_1}, E_{T_2} \geq E_0$ and $|\eta_1 - \eta_2| < .5$, with $\bar{\eta} = (\eta_1 + \eta_2)/2$. The first point to notice is the disagreement between the two sets of theoretical predictions: this arises because the groups do not calculate the same observable due to instabilities in the perturbatively calculated quantity. This is related to the fact that the boundary condition $E_{T_1} = E_{T_2} = E_0$ is an infrared singular point. Typically, in the NLO approximation one needs to consider the production of 3 partons in the final state: it can be separated into two classes:

$$\sigma^{2 \rightarrow 3} = \sigma^{2 \rightarrow 3}(y_c) + \sigma_R^{2 \rightarrow 2}(y_c) \quad (9)$$

with the parameter y_c such that the first term on the right hand side contains events generated with “dangerous” invariant masses [*i.e.* leading to soft and collinear singularities in the matrix element] $s_{ij} > y_c s_{ab}$, while $\sigma_R^{2 \rightarrow 2}(y_c)$ contains events which look like 2-body hard scattering as discussed above. This part contains all divergences and y_c is chosen small enough ($y_c = 10^{-5}$ to 10^{-2}) so that approximations can be used to extract divergences analytically. Upon adding the virtual corrections which are also of type 2 body \rightarrow 2 body scattering all divergences cancel and the theoretical cross section is:

$$\sigma = \sigma^{2 \rightarrow 3}(y_c) + \sigma^{2 \rightarrow 2}(y_c) \quad (10)$$

each piece being regular, the first one being calculated numerically and the second one semi-analytically. By histogramming one reconstructs any observable but it should be checked that the result is independent of y_c . It turns out that for the dijet observable of fig. 5, the condition $E_{T_1}, E_{T_2} > E_0$ introduces constraints on the phase space which spoil the y_c compensation between the terms in the above equation. Harris and Owens [5] (who use a more elaborate method than the one described above) observe that the remaining dependence on y_c is much less than the experimental error bars and present results with some value of y_c while Klasen and Kramer [7] modify the boundary condition to $E_{T_1} > E_0$, allowing for a smaller E_{T_2} if the third unobserved jet has transverse energy less than $E_{T_3} < 1$ GeV. This is sufficient to remove the y_c dependence but the result is rather sensitive to the latter energy cut. As seen in the

Figure 5: *Dijet cross section vs. $\bar{\eta}$ integrated over $E_T^{\text{jet}} > E_0$ for $E_0 = 6, 8, 11, 15$ GeV; the four figs. on the left are as for $x_\gamma > 0.75$; those on the right are for $x_\gamma < 0.75$. The data are from [8]. Thin lines from ref. [5]; thick dashed lines from ref. [7].*

figure this slight modification of the boundary condition considerably affects the predictions [9]. If one considers that the calculation of ref. [5] is closer to the experimental observable there remains a drastic disagreement between the data and the theoretical predictions specially concerning the *resolved* cross section. Disagreement between theory [5, 10, 11] and experiment [12] is also seen when comparing the rapidity distribution of single inclusive jet production as displayed in fig. 6: this is particularly marked at low E_T and large pseudo-rapidities, *i.e.* where the resolved component plays a dominant role. This leads us to the important question of whether or not the theoretical predictions are able to match the experimental observables. Two questions can be raised:

- is it possible to match theoretical jets, made up of partons, with experimental jets reconstructed, via various algorithms, from energy deposited in calorimeter cells?
- how does one take into account the transverse energy of the *underlying event*, *i.e.* the energy generated by the interaction of the *spectator* partons?

The first point was studied many years ago in connection to jet production at the Tevatron [13] and was recently re-analysed in detail for HERA by Kramer and collaborators [14]: the idea is to introduce an extra parameter R_{sep} controlling the width of the jets which is adjusted to fit the data: a better description of the data by the NLO calculations is indeed achieved at the expense, however, of the predictive power of the theory.

Concerning the second point the problem can be qualitatively understood in the following way. At HERA, in events with *direct* photo-production of jets the transverse energy of the *underlying event* is produced by string-like effects: typically a transverse energy of 300 – 400 MeV per unit of rapidity is expected. On the contrary, in resolved photo-production, the rem-

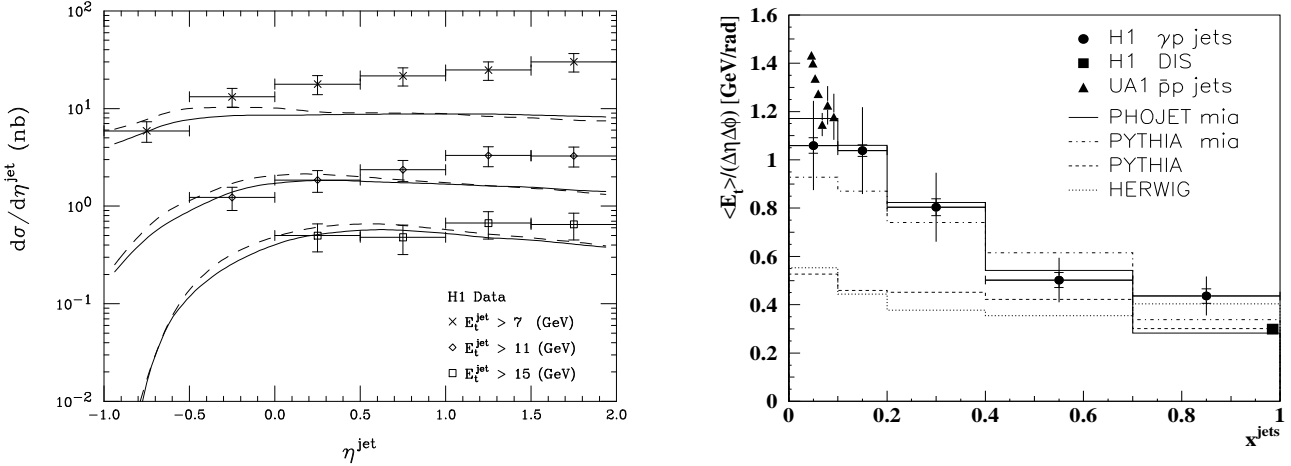


Figure 6: Comparison of the single jet inclusive cross section measured by H1 [12] compared with NLO predictions [5] using 2 different sets of photon structure functions. Transverse energy of the underlying event at HERA as measured by H1 [12].

nants of the photon can undergo soft or semi-hard interactions with those of the proton [15] generating transverse energies in the GeV range: the larger the energy of the photon remnant (*i.e.* the smaller x_γ is) the larger is the underlying transverse energy: this is illustrated in fig. 6 from H1 [12] which shows the E_T outside the jets as a function of x_γ . Such an effect is of course present in purely hadronic reactions but is relatively less important because the much higher E_T values of jets probed in hadronic colliders. On the other hand, jets in $\gamma\gamma$ reactions should be less affected except at very low E_T values ($E_T < 5$ GeV at LEP1) where the *double-resolved* process is dominant. Good agreement of TRISTAN [16, 17] and LEP [18] data with the NLO predictions [19] has been obtained for inclusive two-jet production.

A discussion about the determination of the gluon density in the photon using jet cross sections is given, in the LO approximation, in ref. [3].

A way to avoid problems related to jet definition or to underlying transverse energy is to consider single hadron production. Good agreement is indeed found in photo-production between the NLO predictions [20] and HERA data [21].

4 Charmonium production

There has been new developments concerning the production of hidden heavy flavor at the Tevatron where the usual model predictions, based on the color singlet model, for prompt Ψ production fall an order of magnitude below the experimental results. The interest of HERA lies in the fact, that many of the new parameters introduced in the model can be tested independently. We consider here only the non-diffractive mechanism, corresponding to a Ψ inelasticity factor of $z = p \cdot k_\Psi / p \cdot k_\gamma < .9$. In the factorisation approach of ref. [22] the cross

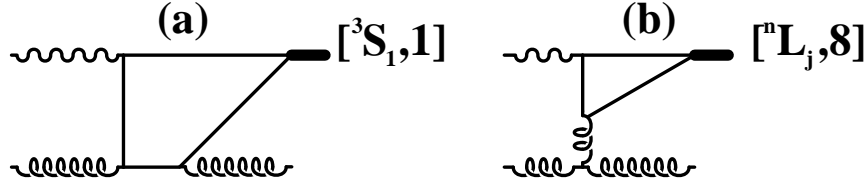


Figure 7: *Some Feynman diagrams for charmonium production. (a): colour singlet production; (b): diagram contributing only to colour octet production.*

section for the production of a heavy quark bound state H is

$$d\sigma(\gamma p \rightarrow HX) = \sum_{[\mathbf{n}]} d\hat{\sigma}(\gamma p \rightarrow Q\bar{Q}[\mathbf{n}]X) < \mathcal{O}^H[\mathbf{n}] >, \quad (11)$$

where $d\hat{\sigma}$ is the cross section for producing a heavy $Q\bar{Q}$ system in state $[\mathbf{n}]$ defined by its color $[\mathbf{1}, \mathbf{8}]$, its spin $[0, 1]$ and orbital angular momentum. This term is calculable perturbatively, the large scale being provided by the heavy quark mass or eventually by the transverse momentum of the system. The factor $< \mathcal{O}^H[\mathbf{n}] >$ describes the non-perturbative transition from the state with quantum numbers $[\mathbf{n}]$ to quarkonium H . Typically $< \mathcal{O}^\Psi[^3S_1, \mathbf{1}] > = 1.16 \text{ GeV}^3$ (from Ψ leptonic decay) while the $\mathbf{8}$ matrix elements $< \mathcal{O}^\Psi[^3S_1, \mathbf{8}] > \sim < \mathcal{O}^\Psi[^3S_0, \mathbf{8}] > \sim < \mathcal{O}^\Psi[^3P_J, \mathbf{8}] > / m_c^2 \sim 10^{-2} \text{ GeV}^3$ as determined from fits to the Tevatron data [23]. The colour $\mathbf{8}$ values are consistent with non-relativistic QCD which predicts their suppression by powers of the velocity of the heavy quark in the bound state [24]. Although the $\mathbf{8}$ matrix elements are small it may happen that the perturbative cross section $d\hat{\sigma}([\mathbf{8}])$ is large so that a non negligible contribution occurs. In the colour $\mathbf{1}$ model the $\mathbf{8}$ matrix elements are assumed to vanish. Many processes contribute to the cross section $d\hat{\sigma}(Q\bar{Q}[\mathbf{n}])$: it is convenient to distinguish fusion processes which are important at small p_T , but are suppressed by a factor m_Q^2/p_T^2 , from fragmentation processes where the $Q\bar{Q}$ state is found in the decay of a Q or gluon jet produced at large transverse momentum. Furthermore, both processes come in the *direct* variety if the photon couples to the hard sub-scattering, or the *resolved* one if the photon structure function is involved. These mechanisms have different z and p_T dependences so that varying the kinematical conditions they could be separated.

Consider first direct fusion processes which should be a good approximation of cross sections at small transverse momentum ($p_T \leq m_Q$) or integrated over p_T . The basic colour singlet diagram is shown in fig. 7a: the heavy $Q\bar{Q}$ pair is produced by photon-gluon fusion and an extra gluon is necessarily emitted so that a $Q\bar{Q}$ state in a $\mathbf{1}$ component can be projected out. NLO corrections to this process have also been calculated [25]. A similar diagram contributes also to the production of a colour $\mathbf{8}$ state together with the diagram of fig. 7b: because of the gluon exchange this diagram will be enhanced near the kinematical region $z \sim 1$. The comparison of the theory [26] with HERA [27, 28] data is shown in fig. 8 where one sees the excellent agreement between data and the colour $\mathbf{1}$ NLO predictions while the $\mathbf{8}$ component seems to yield much too large a contribution at large z values. To claim quantitative disagreement is premature as the non-perturbative $\mathbf{8}$ matrix elements may have been overestimated in the Tevatron analysis; furthermore, doubts have been raised about the validity of the factorisation approach (velocity expansion) in the large z region [30].

The resolved fusion diagrams are easily obtained by substituting to the photon a gluon,

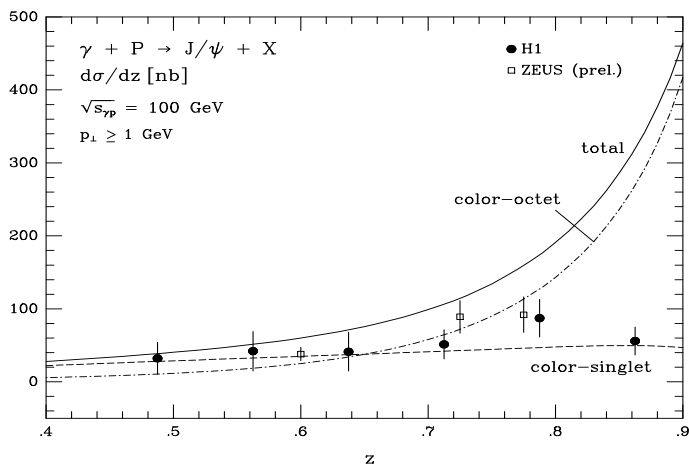


Figure 8: *Fusion contribution to charmonium production at HERA.*

fragment of the photon: obviously this process dominates at small z where it is further found that the **8** contribution overwhelms the **1** one by more than one order of magnitude: thus the region at small p_T , small z or equivalently large rapidity since $z \sim e^{-y_{\text{lab}}}$, should be able to probe the **8** matrix elements.

At large p_T , on the other hand, the production of charmonium in the fragments of a jet should be considered [31, 32]. In the factorisation approach, the fragmentation function of parton i into H takes the form:

$$D_i^H(z, M) = \sum_{[\mathbf{n}]} d_{i \rightarrow c\bar{c}[\mathbf{n}]}(z, M) \langle \mathcal{O}^H[\mathbf{n}] \rangle, \quad i = c, g \quad (12)$$

where the functions d_i are perturbatively calculated (all scales involved are large) and the same non-perturbative matrix elements as above appear. A detailed study at the NLO order [32], including both direct and resolved processes, has recently been performed where it is found an overwhelming dominance of the colour **8** channels at HERA for large y_{lab} and p_T , the more so the larger the γp invariant mass.

The exclusive channel $\gamma p \rightarrow \Psi \gamma$ has also been proposed [33] as a test of the model as it is obviously dominated at large z by the **8** component (see fig. 7a with the final state gluon changed into a photon).

Thus HERA appears a promising place to support or invalidate the colour **8** model if detailed measurements of specific channels can be done over a wide rapidity range for $J\Psi$ production.

Acknowledgements

I am grateful to M. Erdmann for discussions and very helpful advice in the preparation of this talk. I also thank L. Bourhis, I. Butterworth, M. Cacciari, J. Forshaw, J.Ph. Guillet, B.W. Harris, U. Karshon, B. Kniehl, M. Mangano, J.F. Owens and E. Pilon. Support by the EEC program “Human Capital and Mobility”, Network “Physics at High Energy Colliders”, contract CHRX-CT93-0357 (DG 12 COMA), is gratefully acknowledged.

References

- [1] Proceedings of PHOTON '95, D.J. Miller, S.L. Cartwright, V. Khoze *eds.*, World Scientific, Singapore, 1995.
- [2] A. Vogt, these proceedings.
- [3] M. Erdmann, 'The Partonic Structure of the Photon', Springer Tracts in Modern Physics 138, Heidelberg, Springer (1997).
- [4] L. Bourhis, these proceedings; proceedings of the 1995-1996 Workshop for Future Physics at HERA, ed. G. Ingelman.
- [5] B.W. Harris and J.F. Owens, Florida State University preprint FSU-HEP-970411, hep-ph/9704234.
- [6] ZEUS collab., M. Derrick *et al.*, *Phys. Lett. B* **384**, 401 (1996).
- [7] M. Klasen and G. Kramer, hep-ph/9611450, preprint DESY 96-246.
- [8] ZEUS collab., M. Derrick *et al.*, 28th International Conference on High Energy Physics, Warsaw, 1997.
- [9] I thank B.W. Harris and J.F. Owens for a discussion on the differences between the calculations of ref. [5] and ref. [7].
- [10] P. Aurenche, M. Fontannaz, J.Ph. Guillet, *Phys. Lett. B* **338**, 98 (1994).
- [11] D. Bödeker, G. Kramer, S.G. Sales, *Z. Phys. C* **63**, 471 (1994).
- [12] H1 collab, S. Aid *et al.*, *Z. Phys. C* **70**, 17 (1996).
- [13] S.D Ellis, Z. Kunszt, D.E. Soper, *Phys. Rev. Lett.* **69**, 3615 (1992).
- [14] J.M. Butterworth *et al.*, hep-ph/9608481;
M. Klasen and G. Kramer, hep-ph/9701247, preprint DESY-97-002.
- [15] R. Engel, *Z. Phys. C* **66**, 203 (1995);
R. Engel, J. Ranft, *Phys. Rev. D* **52**, 1459 (1995), *D* **54**, 4244 (1996).
- [16] AMY collab., B.J. Kim *et al.*, *Phys. Lett. B* **325**, 248 (1994).
- [17] TOPAZ collab., H. Hayashii *et al.*, *Phys. Lett. B* **314**, 149 (1993).
- [18] OPAL collab., K. Ackerstaff *et al.*, *Z. Phys. C* **73**, 433 (1997).
- [19] P. Aurenche *et al.*, *Prog. Theor. Phys.* **92** 175, (1994);
T. Kleinwort, G. Kramer, hep-ph/9610489, preprint DESY 96-223.
- [20] J. Binnewies, B.A. Kniehl, G. Kramer, *Phys. Rev. D* **52**, 4947 (1995).

- [21] H1 collab., I. Abt *et al.*, *Phys. Lett. B* **328**, 176 (1994);
ZEUS collab., M. Derrick *et al.*, *Z. Phys. C* **67**, 227 (1995).
- [22] G.T. Bodwin, E. Braaten, G.P. Lepage, *Phys. Rev. D* **51**, 1125 (1995).
- [23] P. Cho, A.K. Leibovich, *Phys. Rev. D* **53**, 150 (1996); **D53**, 6203 (1996).
- [24] G.P. Lepage *et al.*, *Phys. Rev. D* **46**, 4052 (1992).
- [25] M. Krämer, *Nucl. Phys. B* **459**, 3 (1996).
- [26] M. Cacciari, M. Krämer, *Phys. Rev. Lett.* **76**, 4128 (1996).
- [27] H1 collab, S. Aid *et al.*, *Nucl. Phys. B* **472**, 3 (1996).
- [28] ZEUS collab., L. Stanco, talk at the International Workshop on Deep Inelastic Scattering, Rome, 1996.
- [29] M. Cacciari, M. Krämer, hep-ph/9609500, Talk given at Workshop on Future Physics at HERA, Hamburg, Germany, 30-31 May 1996.
- [30] M. Beneke, I.Z. Rothstein, M.B. Wise, hep-ph/9705286, preprint CERN-TH/97-86.
- [31] R. Godbole, D.P. Roy, K. Sridhar, *Phys. Lett. B* **373**, 328 (1996).
- [32] B.A. Kniehl, G. Kramer, hep-ph/9702406, preprint DESY 97-012; hep-ph/9703280, preprint DESY 97-036.
- [33] M. Cacciari, M. Greco, M. Krämer, *Phys. Rev. D* **55**, 7126 (1997).

This figure "fig1-1.png" is available in "png" format from:

<http://arxiv.org/ps/hep-ph/9706386v1>